



## Research article

# The transcriptome profiling of diseased mouse aortas discloses a dysregulation of the sympathetic neurotransmission in atherosclerosis

Marco Busnelli<sup>\*,1,2</sup>, Alice Colombo<sup>1</sup>, Stefano Manzini, Elsa Franchi, Giulia Chiesa<sup>\*\*</sup>*Department of Pharmacological and Biomolecular Sciences "Rodolfo Paoletti", Università degli Studi di Milano, Italy*

## A B S T R A C T

Previous reports suggest an association between the development of atherosclerosis and alterations in the aortic sympathetic nervous system, but there is no agreement on whether atherosclerotic plaques are accompanied by increased or decreased sympathetic innervation in the arterial wall.

In the present study, the aortic transcriptional profile of mice with different predisposition to atherosclerosis was investigated to clarify how the expression of genes involved in sympathetic neurotransmission varied.

Eight-week-old C57Bl/6J control mice, Apoe knockout mice (EKO), EKO mice overexpressing human apoA-I (EKO/hA-I) and double Apoe/Apoa1 knockout mice (DKO) mice were fed either a standard rodent diet or a Western-type diet for 22 weeks. Atherosclerosis was quantified, and the aortic transcriptome was analyzed by RNAseq. Western-type diet administration deeply modified the aortic transcriptome. In the genetically modified atherosclerosis-prone mouse lines, an upregulated expression of genes associated with the immunomodulatory response was observed, paralleled by a downregulated expression of the genes related to sympathetic nervous system. Functional enrichment analysis indicated that the presence of advanced atherosclerosis was accompanied by reduced neuronal generation, modulation of synapse chemical transmission, and catecholamine biosynthesis, supporting a relationship between atherosclerosis, dyslipidemia, and sympathetic neurotransmission.

## 1. Introduction

Cardiovascular disease arising from atherosclerosis remains the leading cause of death and morbidity worldwide [1]. The underlying pathology is characterized by a progressive accumulation of lipids and fibrous elements in the large arteries. Atherosclerotic plaques typically develop as asymmetric focal thickenings of the innermost layer of the artery, the intima. Arterial lesions start with the formation of a fatty streak, which is an accumulation of lipid-loaded macrophages in the intimal sub-endothelial space. Fatty streaks then progress into mature, more complex, atherosclerotic plaques: in the centre of the plaque, macrophage foam cells, additional inflammatory cell subsets, dead cells, and extracellular lipid droplets form a core region surrounded by a collagen-rich matrix and a cap of smooth muscle cells [2].

Although much emphasis has been placed on investigating both atherosclerosis onset and progression through subendothelial accumulation of lipids and inflammatory cells, the adventitia - the outer layer of the arteries - may also play a critical role in the progression of the disease [3]. Resident adventitial cells (i.e. fibroblasts, dendritic cells, macrophages, mast cells, progenitor cells, endothelial cells, pericytes) are often the first to be activated and reprogrammed to influence the tone and structure of the vessel wall

\* Corresponding author

\*\* Corresponding author.

E-mail addresses: [marco.busnelli@unimi.it](mailto:marco.busnelli@unimi.it) (M. Busnelli), [giulia.chiesa@unimi.it](mailto:giulia.chiesa@unimi.it) (G. Chiesa).

<sup>1</sup> These authors contributed equally.

<sup>2</sup> Lead contact.

[2]. Moreover, in advanced atherosclerotic plaques, adventitial leukocytes can aggregate in structures resembling lymphoid follicles, termed aortic tertiary lymphoid organs (ATLOs), acting as centres of a local humoral response with B-lymphocyte subset selection, maturation, and antibody production [4,5]. The adventitia also hosts postganglionic sympathetic nerve endings, ramifying into small bundles and forming a plexus. The terminal effector plexus is located near the medial layer, where noradrenergic nerve fibres approach the surface of the smooth muscle cells and establish neuromuscular contact. In general, sympathetic neurons transmit their signal by releasing noradrenaline from their nerve endings; noradrenaline is then capable of spreading through the media, from where it can reach the intima and the endothelium [6–8]. Recent evidence seems to suggest that in the adventitia of diseased arteries, an increased amount of immune cells associates with a more abundant sympathetic innervation [9]. This finding is in contrast to what has been observed in previous studies, conducted in a variety of experimental settings and different animal models, in which a reduction in sympathetic markers/functionality was observed following the administration of diets that could promote atherosclerosis development [10–13].

Relying on the aortic transcriptional profile of mice with different predisposition to atherosclerosis, the present study was set to clarify whether, and how, the expression of genes involved in sympathetic neurotransmission varied.

To this aim, C57Bl/6J control mice (Bl/6), hyperlipidemic atherosclerosis-prone Apoe knockout mice (EKO), double Apoe/Apoa1 knockout mice (DKO) and EKO mice overexpressing human apoA-I (EKO/hA-I) were fed a standard rodent diet (SRD), poor in lipids and with no cholesterol, or a Western-type diet (WD), enriched in saturated fatty acids and cholesterol.

We provide evidence that the administration of a lipid-rich diet to dyslipidemic mouse models is associated with a reduced expression of genes attributable to sympathetic nervous system activity when atherosclerosis develops in the aorta.

## 2. STAR methods

### Key resources table.

REAGENT or RESOURCE	SOURCE	IDENTIFIER
<b>Reagents and kits</b>		
Diet: standard rodent chow	Mucedola	4RF21
Diet: Western-type	Envigo	TD.88137
Isoflurane	Merial	N01AB06
Haematoxtlin	Bio-Optica	05–06002
Eosin	Bio-Optica	05–10003
NucleoSpin RNA columns	Macherey-Nagel	740955.50S
Trizol	Invitrogen	Cat. no.: 15596026
<b>Experimental models: Organisms/Strains</b>		
Mouse: C57BL6/J	JAX/Charles River Laboratories	Strain #:000664 (RRID: IMSR_JAX:000664)
Mouse: EKO	JAX/Charles River Laboratories	Strain #:002052 (RRID: IMSR_JAX:002052)
Mouse: EKO/hA-I	In house	Reference: [14]
Mouse: DKO	In house	Reference: [15]
<b>Deposited data</b>		
Fastq files	NCBI GEO	GSE163657, GSE173974
<b>Software and Algorithms</b>		
cutAdapt	(Martin, 2011)	<a href="https://cutadapt.readthedocs.io/en/stable/">https://cutadapt.readthedocs.io/en/stable/</a>
bowtie	(Langmead, 2010)	<a href="https://bowtie-bio.sourceforge.net/index.shtml">https://bowtie-bio.sourceforge.net/index.shtml</a>
DAVID	(Sherman et al., 2022)	<a href="https://david.ncifcrf.gov/">https://david.ncifcrf.gov/</a>
DESeq2	(Love et al., 2014)	<a href="https://bioconductor.org/packages/release/bioc/html/DESeq2.html">https://bioconductor.org/packages/release/bioc/html/DESeq2.html</a>
ImageJ	(Schneider et al., 2012)	<a href="https://imagej.net/ij/download.html">https://imagej.net/ij/download.html</a>
Prism	GraphPad	<a href="https://www.graphpad.com/">https://www.graphpad.com/</a>
reString	(Manzini et al., 2021)	<a href="https://github.com/Stemanz/restring">https://github.com/Stemanz/restring</a>
STRING	(Szklarczyk et al., 2015)	<a href="https://string-db.org/">https://string-db.org/</a>
Trimmomatic	(Bolger et al., 2014)	<a href="http://www.usadellab.org/cms/?page=trimmomatic">http://www.usadellab.org/cms/?page=trimmomatic</a>
NDP.view2	Hamamatsu Photonics	<a href="https://www.hamamatsu.com/jp/en/product/life-science-and-medical-systems/digital-slide-scanner/U12388-01.html">https://www.hamamatsu.com/jp/en/product/life-science-and-medical-systems/digital-slide-scanner/U12388-01.html</a>

## 3. Resource availability

### 3.1. Lead contact

Further information and requests for resources should be directed to and will be fulfilled by the lead contact, Marco Busnelli ([marco.busnelli@unimi.it](mailto:marco.busnelli@unimi.it)).

### 3.2. Materials availability

This study did not generate new unique reagents.

## 4. Materials and methods

**Animals and diets.** Procedures involving animals and their care were conducted in accordance with institutional guidelines that are in compliance with national (D.L. No. 26, March 4, 2014, G.U. No. 61 March 14, 2014) and international laws and policies (EEC Council Directive 2010/63, September 22, 2010: Guide for the Care and Use of Laboratory Animals, United States National Research Council, 2011). The experimental protocol was approved by the Italian Ministry of Health (Protocollo 2012/4).

Eight-week-old C57BL/6J (Bl/6; RRID: IMSR\_JAX:000664) and EKO mice (strain 002052; RRID: IMSR\_JAX:002052) were purchased from Charles River Laboratories (Calco, Italy). ApoE/apoA1 double knockout mice (DKO) were previously generated in our lab [14]. EKO/hA-I were obtained by multiple crosses between EKO mice and hemizygous mice overexpressing human apoA-I [15].

Primers specific for murine ApoE and ApoA1 and human APOA1 were used to screen genotypes [14].

Mice were maintained under standard laboratory conditions (12-h light cycle, temperature 22 °C, humidity 55 %), with free access to standard rodent diet (SRD, 4RF21, Mucedola, Settimo Milanese, Italy) or Western-type diet (WD, TD.88137, Harlan Laboratories, Italy) for 22 weeks. Only male mice were enrolled in the study, to prevent the possible impact of hormonal changes of female mice on the results.

**Harvesting of the aorta.** At the end of the dietary treatments, 30-week-old mice were sacrificed under general anesthesia with 4 % isoflurane (Merial Animal Health, Woking, UK) and blood was removed by perfusion with 1 × phosphate-buffered saline (PBS). Briefly, mice were euthanized by exsanguination under general anesthesia with 2 % isoflurane (Merial Animal Health, Woking, UK), where blood was removed by perfusion with 1 × PBS. Aortas were then snap-frozen in liquid nitrogen for RNA-seq analyses (n = 3), or rapidly dissected from the aortic root to the iliac bifurcation and, after removal of the periadventitial fat, were longitudinally opened, pinned flat on a black wax surface in ice-cold PBS and photographed unstained for plaque quantification (n = 3–9). Aorta images were captured with a stereomicroscope-dedicated camera (IC80 HD camera, MZ6 microscope, Leica Microsystems, Germany) and analyzed with ImageJ [16]. Two independent operators, blinded to the dietary treatments, quantified atherosclerosis extent as percentage of area covered by plaque [17,18].

**RNA extraction.** Total RNA was isolated from mouse aorta and extracted as previously described [19]. RNA was quantified and checked, and 1 µg RNA was retrotranscribed to cDNA. Possible gDNA contamination was ruled out as described [18]. Data sets can be accessed at NCBI (Gene Expression Omnibus) GSE163657 [20], and GSE173974 [21].

**RNA-Seq Analysis.** For RNA-seq analysis, the quality of the mRNA was tested using the Agilent 2100 Bioanalyzer (Agilent Technologies, CA), and only libraries with RNA integrity number  $\geq 7$  were included. RNA samples were processed using the RNA-seq Sample Prep kit from Illumina (Illumina, Inc, CA). Eight to 9 tagged libraries were loaded on one lane of an Illumina flowcell, and clusters were created using the Illumina Cluster Station (Illumina, Inc, CA). Clusters were sequenced on a Genome Analyzer IIX (Illumina, Inc, CA) to produce 50 nt single-reads.

**qPCR.** Twenty nanograms of cDNA were used as template for each quantitative polymerase chain reaction, performed for 40 cycles on a CFX Connect thermal cycler, with iTAQ Universal Sybr Green Supermix (Bio-Rad, Segrate, Italy). Conditions and primers are detailed in Fig. S1. The specificity of amplicons was verified by melting curve analysis. Fold changes, relative to the control group, were calculated with the  $\Delta\Delta C_t$  method [22]. The gene cyclophilin A (Ppia) was used as reference gene.

**Preprocessing of Reads.** Raw sequence reads were trimmed using Trimmomatic software [23], and applying the leading, trailing, and sliding windows operations, with the following quality score cutoffs, respectively:  $Q_s \geq 15$ ,  $Q_s \geq 10$ , and average  $Q_s \geq 15$ .

**Differential Gene Expression.** Transcript abundance estimation and differential expression analyses were performed using the standard Bowtie-Tophat-Cuffdiff pipeline on the Refseq annotation of the mm10 mouse reference genome assembly. Transcriptome assembly functions of cufflinks were deactivated and only established transcripts annotations were used [24].

Differential expression analyses were executed by performing direct pairwise comparisons between the conditions under study. A false discovery rate cutoff value of 0.05 was applied for the identification of differentially expressed genes. Functional enrichment analyses were performed with String-DB [25] (version 11.5) and reString (version 0.1.18) [21]. In order to further confirm the robustness of the findings obtained, particularly with regard to the enrichment of biological processes referable to neurotransmission, the DAVID database was also used [26].

**Statistical Analyses.** Analyses were performed with GraphPad Prism version 8.2.1. Significant differences were determined by ANOVA followed by Tukey post hoc test or by Kruskal-Wallis followed by Dunn post hoc test, or where appropriate, by unpaired Student's t-test or by unpaired Mann-Whitney's *U* test according to the check of normality of residuals (Shapiro-Wilk test).

## 5. Results

### 5.1. The aortic gene expression profile in atherosclerosis-prone mice fed WD shows activation of the immune response and suppression of the catecholaminergic neurotransmission

As previously described, EKO/A-I, EKO and DKO mice are characterized by a dyslipidemic condition, the former with elevated HDL and apoA-I levels, the latter with an almost complete lack of HDL particles [15,20]. WD administration strongly increases plasma cholesterol levels in the three mouse lines [20,21].

On SRD, aortic atherosclerosis was detected only in DKO and EKO mice, with the area of the whole aorta covered by plaques being  $2.03 \pm 1.83\%$  and  $2.70 \pm 2.17\%$ , respectively. On WD, aortic plaques developed in all genotypes. Plaque extent along the entire aorta was  $7.77 \pm 4.61\%$  in EKO/hA-I,  $16.45 \pm 9.95\%$  in DKO and  $31.66 \pm 6.55\%$  in EKO. No plaque development was ever observed in Bl/6 mice (Fig. 1A–H and Fig. S2).

The effect of SRD and WD on the aortic gene expression profile of each mouse line was analyzed. Transcript abundance estimation was validated by quantitative polymerase chain reaction on 6 relevant genes and was found to closely match RNA-seq results (Figs. S3–S4). The three genotypes showed a variable number of differentially expressed genes, considering the comparison between the two dietary treatments (394 in EKO/hA-I, 226 in DKO, 862 in EKO). Among those, upregulated genes on WD (194 in EKO/hA-I, 196 in DKO, 548 in EKO) were mainly attributable to both an enhanced immunoinflammatory response and an increased presence of

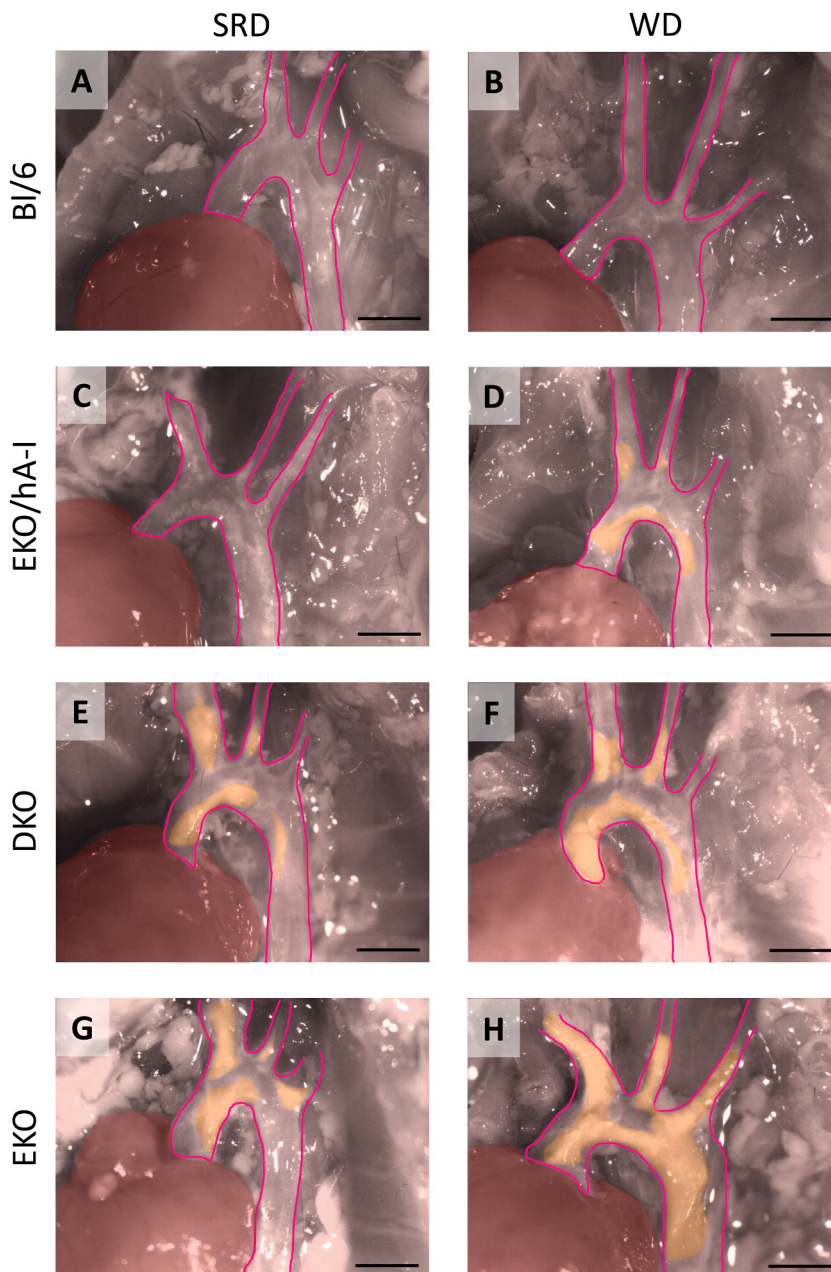
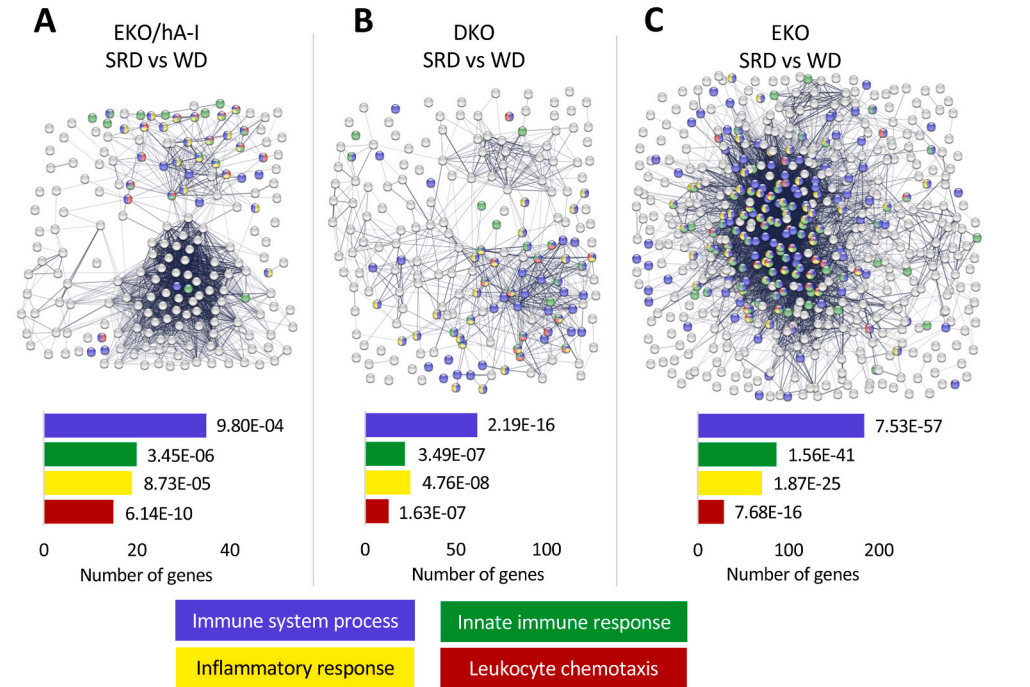


**Fig. 1.** Representative images of the aortic arch originating from the heart. The aortic arch of the different mouse models described in the study at the end of the two dietary treatments is shown, being the district with most plaque development: Bl/6 (A, B), EKO/hA-I (C, D), DKO (E, F), EKO (G, H). The aorta and supra-aortic vessels are outlined by the pink line; plaques are highlighted by the orange areas; the heart is highlighted by the red areas. Scale bar: 2 mm.

leukocytes (GO:0002376 Immune system process; GO:0045087 Innate Immune response; GO:0006954 Inflammatory response; GO:0030595 Leukocyte chemotaxis) (Fig. 2A–C). Among the genes whose expression was reduced following WD, a considerable amount in EKO/hA-I (over 70 out of 200 transcripts) was involved in the neuronal compartment and synaptic signal transmission. The

**UPREGULATED BIOLOGICAL PROCESSES IN ATHEROSCLEROSIS-PRONE GENOTYPES ON WD**



**DOWNREGULATED BIOLOGICAL PROCESSES IN ATHEROSCLEROSIS-PRONE GENOTYPES ON WD**

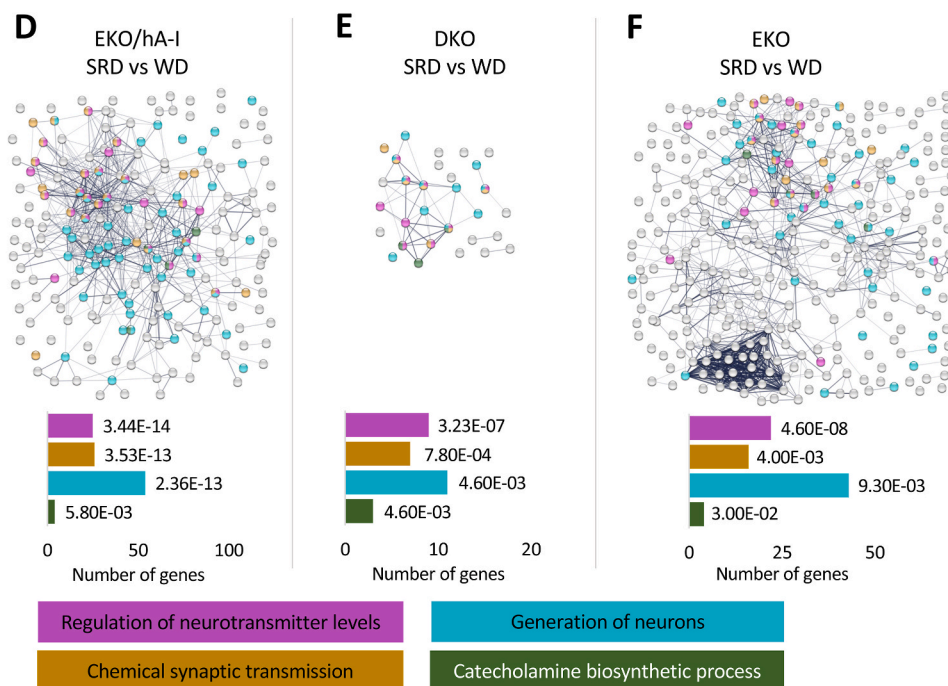


**Fig. 2. Biological processes enriched by diet-modulated genes in the aortas of EKO/hA-I, DKO and EKO mice.** The most relevant biological processes enriched by upregulated and downregulated genes when comparing the two dietary treatments are reported for EKO/hA-I mice (A, D), DKO mice (B, E) and EKO mice (C, F). The enriched GO Terms - Biological Processes were determined and visualized by String-DB.

evaluation of Gene Ontology (GO) Biological Processes allowed this observation to be appreciated (GO:0001505 Regulation of neurotransmitter levels; GO:0007268 Chemical synaptic transmission; GO:0048699 Generation of neurons; GO:0042423 Catecholamine biosynthetic process) (Fig. 2D and Fig. S5A). In DKO mice, a limited number of genes with reduced expression in WD was observed, but again 17 out of 30 genes allowed an enrichment similar to that observed in EKO/hA-I mice (Fig. 2E and Fig. S5B). Finally, EKO mice also showed significantly reduced expression of genes involved in neurotransmission pathways when fed WD (about 60 out of 314) (Fig. 2F and Fig. S5C).

The search for common differentially expressed genes in the above comparisons revealed that 26 upregulated genes on WD were shared among EKO/hA-I, DKO and EKO and were related to the immunoinflammatory response (Fig. 3A–C and Fig. S6).

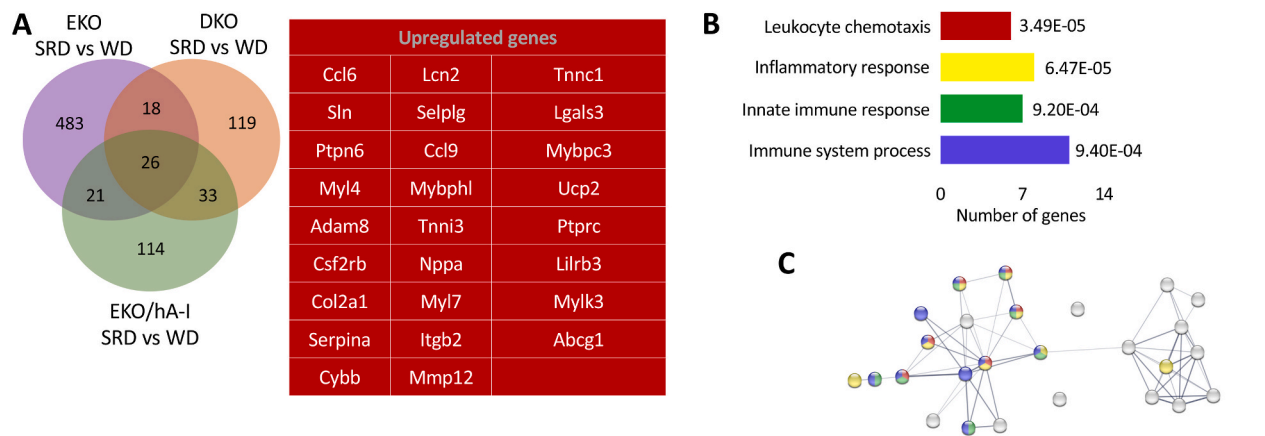
The five genes whose expression increased most consistently on WD, based on p-value, were Col2a1, Lcn2, Mmp12, Mybpc3 and Sln, mutually independent genes involved in immune response, matrix remodeling, and muscle cell activity (Fig. S7A).

Conversely, the genes whose expression decreased in all the genotypes were 21, mostly belonging to neurotransmission-related biological processes (Fig. 3D–F and Fig. S8).

The five genes whose expression decreased most consistently on WD based on p-value were Slc6a2, Dbh, Th, Ddc and Syt4. Slc6a2 encodes for a membrane transporter responsible for noradrenaline reuptake that acts as a regulator of noradrenaline homeostasis. Dbh, Th and Ddc are the genes coding for the three enzymes involved in noradrenaline synthesis, whereas Syt4 encodes for a regulator of catecholamine secretion (Fig. S7B).

The functional enrichments evaluated by other pathway databases (i.e., Gene Ontology – Cellular Component, Reactome, The Mammalian Phenotype Ontology) suggested that upregulated genes were mainly involved in muscle contraction and immune response (Figs. S9A–C). Downregulated genes were instead involved in catecholamine synthesis and nervous signal transmission, their cellular localization being almost entirely confined to the neuron and the synapse (Figs. S9D–F).

**UPREGULATED BIOLOGICAL PROCESSES IN EKO/hA-I, DKO AND EKO MICE FED WD vs SRD**



**DOWNREGULATED BIOLOGICAL PROCESSES IN EKO/hA-I, DKO AND EKO MICE FED WD vs SRD**

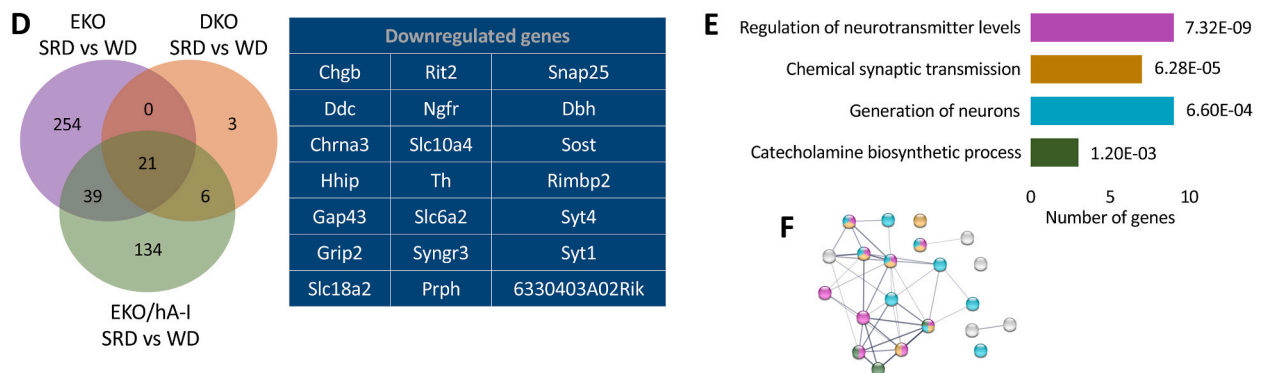
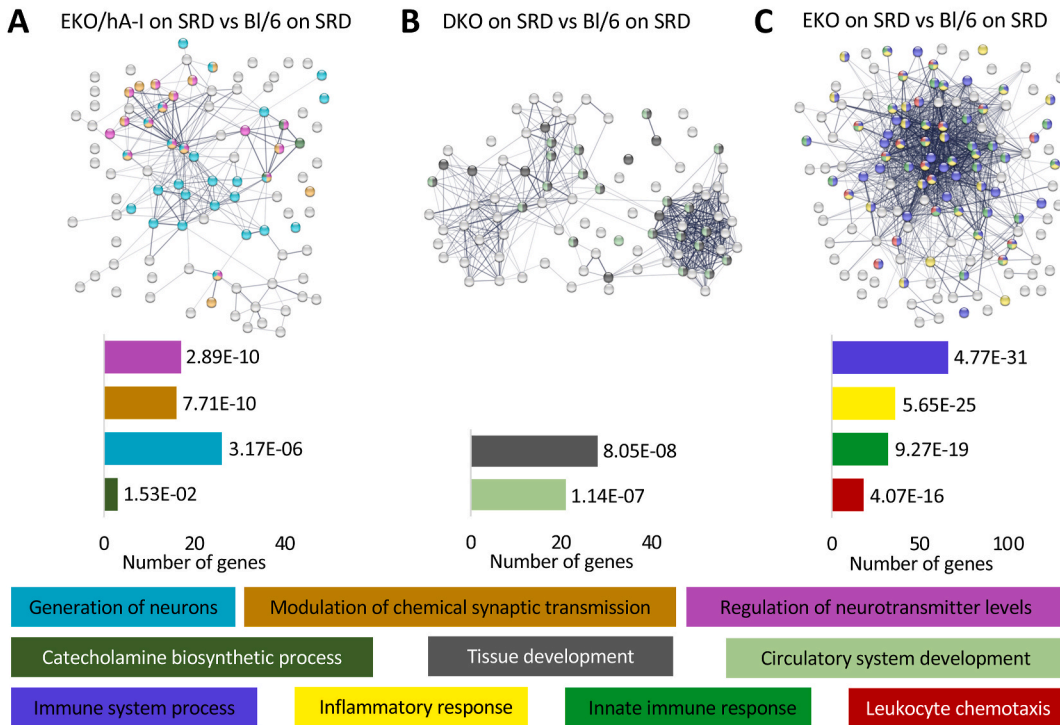


**Fig. 3. Shared upregulated and downregulated genes in WD-fed atherosclerosis-prone genotypes.** EKO/hA-I, DKO and EKO mice shared 26 upregulated genes when fed WD vs SRD (A). According to String-DB, the corresponding enriched GO Terms - Biological Processes were involved in the immunoinflammatory response (B, C). The same three genotypes shared 21 downregulated genes when fed WD vs SRD (D), mostly belonging to neurotransmission-related biological processes (E, F).

5.2. Reduced expression of genes involved in catecholaminergic neurotransmission is associated to the development of atherosclerotic plaques in the aorta

To understand to which extent the genetic background could influence the aortic gene expression profile, the transcriptome of Bl/6

**UPREGULATED GENE ONTOLOGY TERMS - BIOLOGICAL PROCESS**



**DOWNREGULATED GENE ONTOLOGY TERMS - BIOLOGICAL PROCESS**

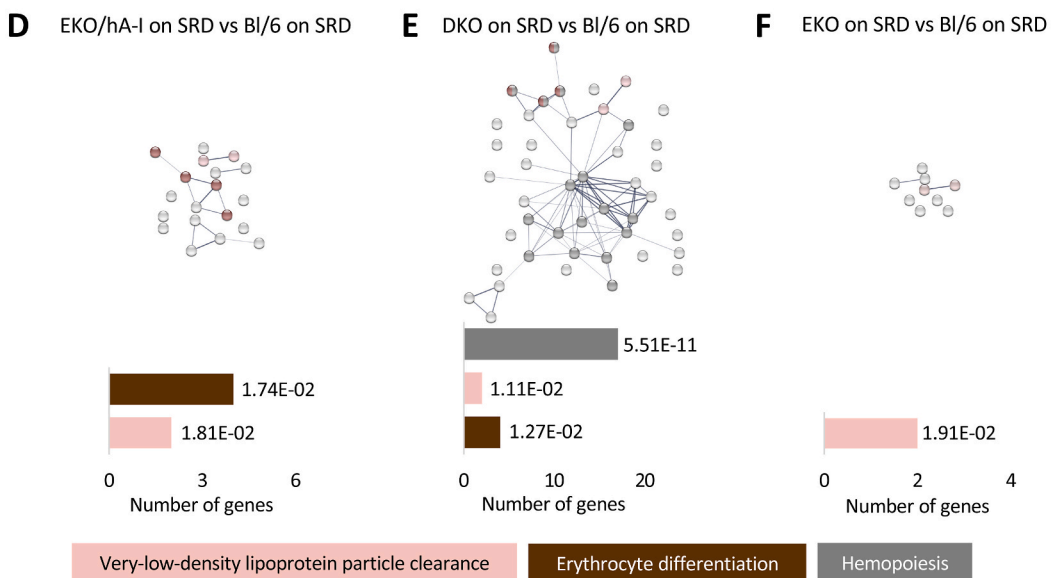
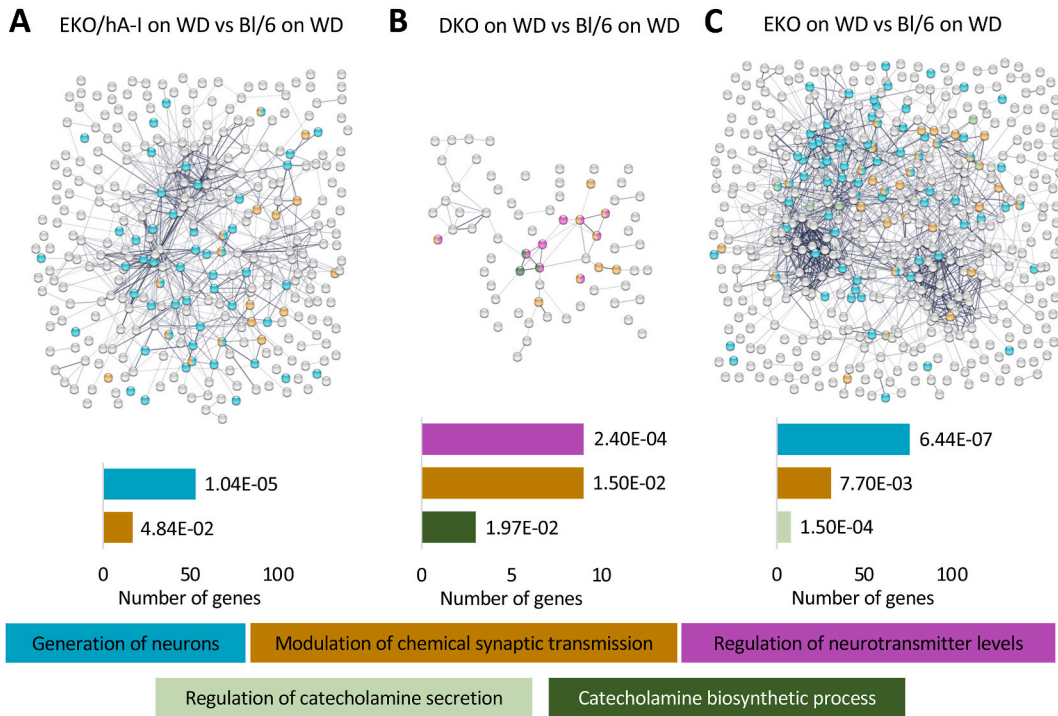


**Fig. 4. Biological processes enriched by genotype-modulated genes in the aortas of EKO/hA-I, DKO and EKO mice vs Bl/6 mice fed SRD.** The most relevant biological processes enriched by upregulated and downregulated genes when comparing Bl/6 mice with EKO/hA-I mice (A, D), DKO mice (B, E) and EKO mice (C, F) are reported. The enriched GO Terms - Biological Processes were determined and visualized by String-DB.

control mice fed SRD was compared, in turn, with the transcriptome of every other genotype fed the same diet. In EKO/hA-I mice, 97 genes were upregulated, mostly involved in neurotransmission (GO:0001505 Regulation of neurotransmitter levels; GO:0007268 Modulation of chemical synaptic transmission; GO:0048699 Generation of neurons; GO:0042423 Catecholamine biosynthetic process)

**DOWNREGULATED BIOLOGICAL PROCESSES**



**DOWNREGULATED CELLULAR COMPONENTS**

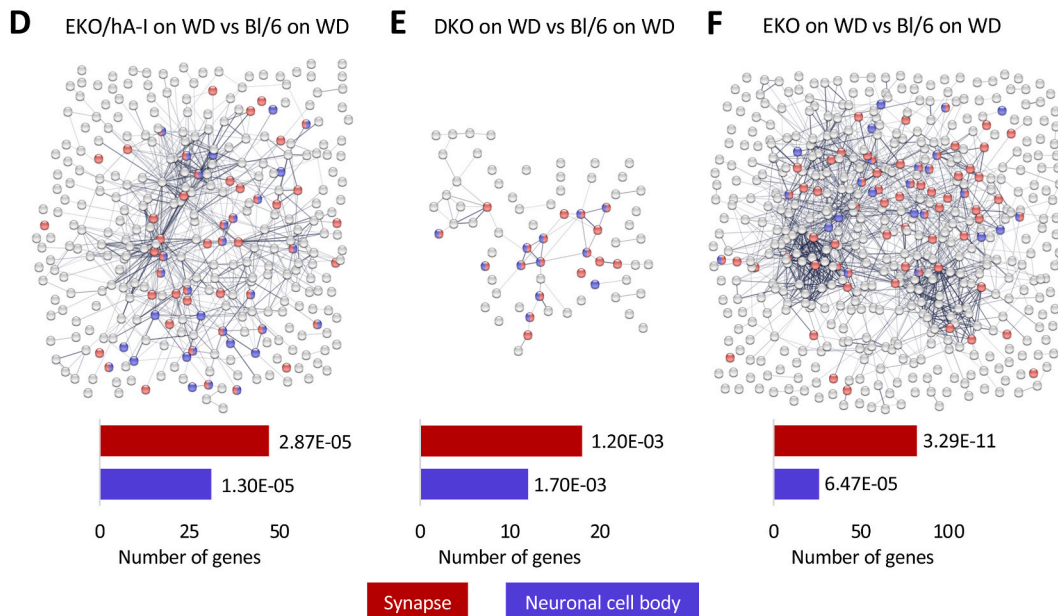


**Fig. 5. Biological processes and cellular components enriched by downregulated genes in the aortas of EKO/hA-I, DKO and EKO mice vs Bl/6 mice fed WD.** The most relevant biological processes and cellular components enriched by downregulated genes in atherosclerosis-prone mice vs Bl/6 mice on WD are reported: EKO/hA-I vs Bl/6 (A, D), DKO vs Bl/6 (B, E), EKO vs Bl/6 (C, F). The enriched GO Terms were determined and visualized by String-DB.

(Fig. 4A). In DKO, the 89 genes showing an increased expression were involved in Tissue development (GO:0009888) and Circulatory system development (GO:0072359) (Fig. 4B). EKO mice displayed an increased expression of 134 genes, mostly belonging to immunoinflammatory pathways (GO:0002376 Immune system process; GO:0006954 Inflammatory response; GO:0045087 Innate Immune response; GO:0030595 Leukocyte chemotaxis) (Fig. 4C). In all comparisons, a low number of downregulated genes was detected and the Very-low-density lipoprotein particle clearance (GO:0034447) was the only biological process constantly altered (Fig. 4D–F).

Differently from EKO/hA-I, DKO and EKO mice, Bl/6 mice respond to WD with a moderate elevation of plasma cholesterol levels and do not develop atherosclerotic plaques [20]. The aortic transcriptional profile of SRD- vs WD-fed Bl/6 mice showed only 34 differentially expressed genes, which do not enrich any biological process (data not shown). The aortic transcriptome of EKO/hA-I, DKO and EKO on WD was then compared with that of Bl/6 mice on the same diet. The transcriptome of each of the three atherosclerosis-prone genotypes was again characterized by an increased expression of genes related to immunoinflammation (data not shown) and a reduced expression of genes belonging to the synaptic neurotransmission (Fig. 5A–F), suggesting that these changes occur when atherosclerosis develops (Fig. 6A–B).

## 6. Discussion

A growing body of evidence suggests that an interaction may occur between the development of atherosclerosis and alterations in the sympathetic nervous system innervating the aorta. The peripheral nervous system uses the adventitia to reach the vessels. Neither the intima nor the media in the arteries are innervated by axon endings, and the same applies to atherosclerotic plaques [27]. Evidence from a recent study, aimed at investigating the crosstalk between the atherosclerotic aorta and the peripheral nervous system, suggested that the axon density was markedly higher in the adventitia located in the proximity of advanced atherosclerotic plaques of EKO

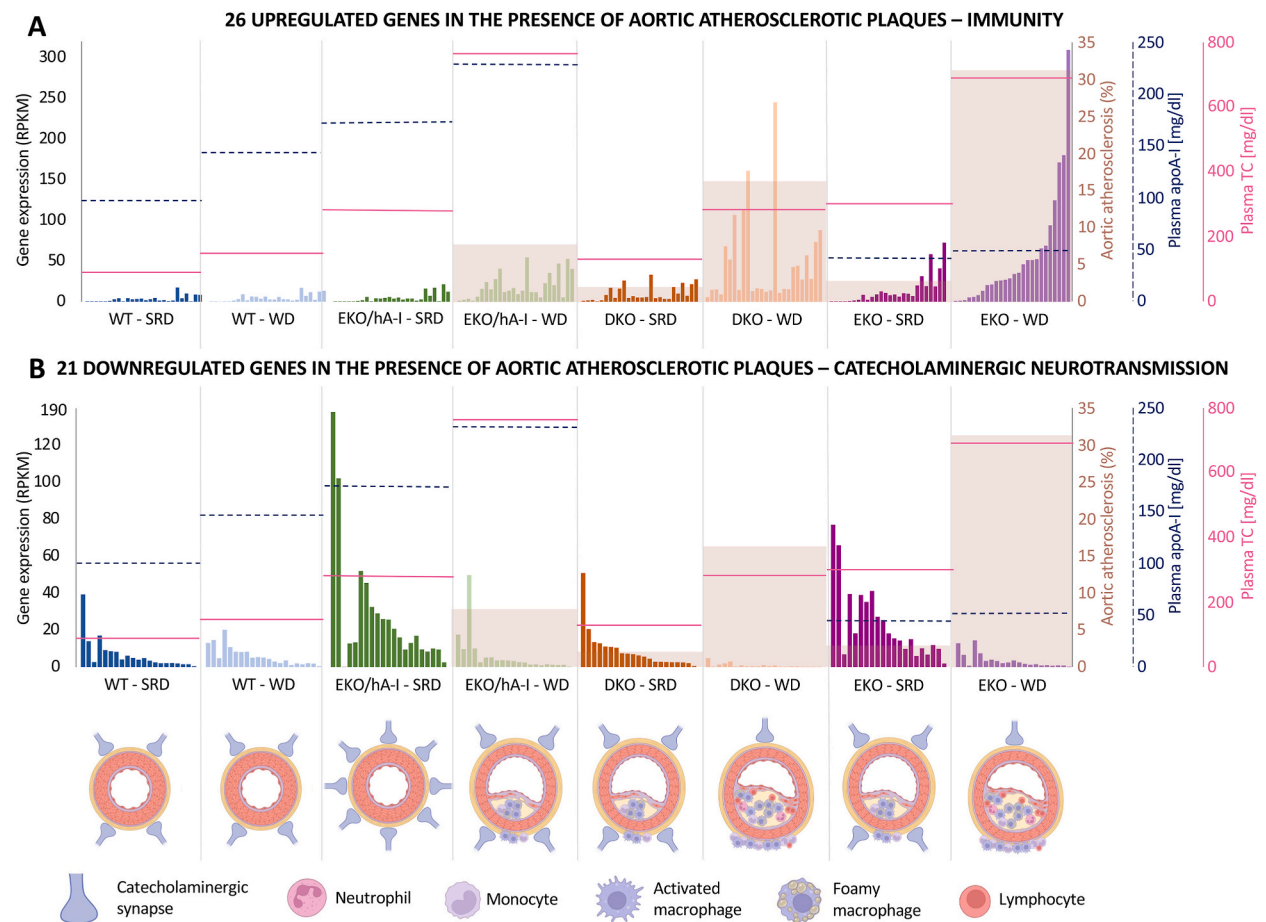


**Fig. 6. Synopsis of main results and working hypothesis.** Trend of the 26 genes whose expression is always increased on WD vs SRD in atherosclerosis-prone genotypes (A). Trend of the 21 genes whose expression is always reduced on WD vs SRD in atherosclerosis-prone genotypes (B). WT: Bl/6 mice. Gene expression levels are reported (Reads per kilobase of transcript per million reads mapped, RPKM) and related to plaque development expressed as % of aortic surface area covered by plaques (gray boxes), plasma levels of apoA-I (mg/dl; blue dotted line), and plasma levels of total cholesterol (mg/dl; violet line).

mice, than in the adventitia next to healthy aortic segments [9].

To investigate the pathogenesis of atheroma in this regard, in the present study, plaque development and gene expression profile of aortas were evaluated in three mouse models, differing for dyslipidemic condition and atherosclerosis susceptibility. Specifically, EKO mice, the gold standard mouse model of atherosclerosis, are hypercholesterolemic and prone to develop lesions in several arterial districts even on standard rodent diet [28], EKO/hA-I mice are hyperlipidemic and characterized by elevated apoA-I and HDL plasma concentrations, which confer a lower propensity to atherosclerosis development, DKO mice lack both apolipoprotein E and apolipoprotein A-I, and therefore they are almost completely devoid of HDL and very prone to atherosclerosis. To widen the experimental setting, two dietary conditions were investigated: a standard rodent diet (SRD) and a Western diet (WD), this latter able to aggravate hyperlipidemia and accelerate atherosclerosis in these models. Indeed, whereas on SRD no atherosclerosis was detectable in EKO/hA-I aortas and a moderate plaque development was observed in both EKO and DKO, WD led to atherosclerosis development in EKO/hA-I and strongly worsened that in EKO and DKO.

The gene expression profile of the whole aortas, harvested after 22 weeks of the two dietary treatments, was investigated by a high-throughput sequencing approach.

The administration of WD, compared to SRD, deeply modified the aortic transcriptome. Whereas the upregulation of genes associated to the immunomodulatory response was somehow expected, being well known the role of the immune response in the onset and development of atherosclerosis, of particular interest was the observation of a downregulation of genes involved in neurotransmission across the synapse and a concomitant reduction in catecholamine biosynthesis, which suggest a compromised signalling of the sympathetic nervous system. This result was strengthened by the finding of common genes up and downregulated in the three mouse lines fed WD.

To evaluate if an alteration in neurotransmission was somehow intrinsic to the lack of apoE, which is the genetic condition shared by the three mouse lines investigated, the aortic transcriptome of Bl/6 mice fed SRD was compared to that of EKO/hA-I, EKO and DKO mice on the same diet. No DE genes involved in neurotransmission were found in the comparison of Bl/6 with both EKO and DKO mice, suggesting that a perturbation of neurotransmission is not a consequence of the genotype itself. Interestingly, SRD-fed EKO/hA-I mice, characterized by elevated HDL and atherosclerosis resistant, showed an upregulation of the neurotransmission genes compared to Bl/6 mice. Altogether, the data above described are suggestive of an active synaptic neurotransmission as a condition associated with healthy vessels, and a downregulation of neurotransmission as associated to atherosclerosis development. Additionally, the results also seem to suggest a link among elevated apoA-I levels, atherosclerosis resistance and activated neurotransmission, which will need further investigations.

The observation of a downregulated neurotransmission in atherosclerotic aortas is apparently in contrast with the increased axon density recently observed in the aortic adventitia in the proximity of plaques, where both the accumulation of immune cell aggregates - forming the so-called ATLOs (artery tertiary lymphoid organs) - and a higher synaptic activity were observed [9]. In the present study we did not perform a morphological analysis of the vessels, thus we cannot add this piece of information to our data. However, it should be noted that Mohanta et al. [9] observed an increased axon density primarily in aged EKO mice (78 weeks of age) and to a much lower degree at earlier ages, including that of the mice of our study. Altogether these and our data seem to suggest a dynamic synaptic plasticity during atherosclerosis development, that depends on genotype, age and diet.

Actually, the interplay between hyperlipidemia, atherosclerosis and sympathetic neurotransmission has been the object of several previous investigations that have evaluated the impact of elevated plasma lipids on the response of the arterial wall to catecholamines. Studies in rabbits have demonstrated that both dietary- and genetically-induced hypercholesterolemia impairs the arterial contractility as a consequence of a reduced release of endogenous noradrenaline [10,11]. In addition, a cholesterol-supplemented diet to rats increased by three-fold plasma cholesterol levels and attenuated the sympathetic noradrenergic neurotransmission in the tail artery, reducing its noradrenaline content [12].

It is well known that hyperlipidemia, and particularly hypercholesterolemia, is the main driver of atherosclerosis development in animal models [29], and a major risk factor in humans [30], leading to lipid deposition in the arterial wall. This condition makes it difficult to establish if the lower sympathetic activity observed in hypercholesterolemic experimental models is a consequence of the hyperlipidemia, or it is determined by the alterations of the arterial wall arising from the formation of atherosclerotic plaques.

Data obtained in this study do not completely clarify this scenario, but the simultaneous evaluation of multiple genotypes with varying degrees of dyslipidemia may authorize some speculations. SRD-fed EKO and WD-fed DKO mice display comparable plasma cholesterol levels, but they are characterized by a very different degree of atherosclerosis, which is very low in EKO and quite relevant in DKO (Fig. 2). Interestingly, the sympathetic activity is high in SRD-fed EKO mice and low in WD-fed DKO, suggesting that its regulation is driven by plaque formation, rather than by hypercholesterolemia. On the other hand, extremely high cholesterol levels, as those observed in EKO/hA-I fed WD, cause only a moderate atherosclerosis development, but dramatically downregulate the expression of genes involved in neurotransmission.

Taken together, our data seem to suggest that aortic sympathetic neurotransmission is impaired in arteries affected by severe atherosclerosis, but also that a dramatic hypercholesterolemia can itself drive this alteration. Interestingly, previous studies have shown that a reduced sympathetic neurotransmission can contribute to atherosclerosis worsening. Sympathectomy in cholesterol-fed rabbits made aortas more susceptible to atherosclerosis development than those of fully innervated controls [31–33]. Similar results have been achieved in rats, where the combination of sympathectomy and hypercholesterolemia led to a marked cholesterol accumulation in the arterial wall [34,35].

In conclusion, the transcriptome profile of aortas from different mouse models shows that, alongside the well-known role of inflammation and immune response, a relationship exists between atherosclerosis, dyslipidemia and sympathetic neurotransmission.

## 7. Limitations of the study

The present work was inspired by some relevant evidence from the literature in which a possible role played by sympathetic innervation in atherosclerosis was highlighted. It was therefore decided to scan gene expression datasets obtained from the aortas of mouse models with different susceptibility to atherosclerosis development, as well as from atherosclerosis-resistant control mice, with particular emphasis on neuronal markers. The data consistently showed, in diseased aortas of multiple genotypes, a robust down-regulation of genes related to sympathetic innervation, both neuronal/synaptic markers and catecholaminergic markers.

The observations achieved solely at the transcriptomic level in the whole aorta certainly represents a limitation of the study. However, this initial evaluation was primarily intended to better assess if/how many possible neuronal targets were involved in atherosclerosis.

Defining the mechanism underlying the alteration of sympathetic innervation during vascular lesion formation will require structured studies integrating expertise in vascular pathophysiology and neurobiology. It will be important to discriminate how innervation varies in arterial districts with abundant plaque formation (i.e., the aortic arch), compared with districts without or with less plaques (i.e., the thoracic aorta). Moving beyond gene expression, it will be critical to understand whether and how the sympathetic innervation changes, at the functional level, during atherosclerosis progression from the healthy arterial wall to the overt lesion.

## Data and code availability

- This paper has produced and made publicly available RNAseq data. The Gene Expression Omnibus (GEO) accession number is listed in the key resources table.
- Any additional information required to reanalyze the data reported in this paper is available from the lead contact upon request.

## Inclusion and diversity

We support inclusive, diverse, and equitable conduct of research.

## CRediT authorship contribution statement

**Marco Busnelli:** Writing – original draft, Visualization, Investigation, Funding acquisition, Formal analysis, Conceptualization. **Alice Colombo:** Writing – original draft, Investigation, Formal analysis. **Stefano Manzini:** Writing – original draft, Software, Investigation, Formal analysis, Conceptualization. **Elsa Franchi:** Visualization, Investigation. **Giulia Chiesa:** Supervision, Resources, Project administration, Funding acquisition, Conceptualization.

## Declaration of competing interest

The authors declare that they have no known competing financial interests or personal relationships that could have appeared to influence the work reported in this paper.

## Acknowledgements

This project has received funding from the European Union's Horizon Europe research and innovation programme under Grant Agreement no. 101057724 - LiverTarget (G. Chiesa) and from the European Union's Horizon 2020 research and innovation programme under the ERA-Net Cofund action no. 727565 (OCTOPUS project) and the MIUR (G. Chiesa). This project was also supported by Piano Sostegno alla Ricerca (PSR) 2021 Linea 2 and PSR2022 Linea 2 from Università degli Studi di Milano (M. Busnelli).

We are in debt to Elda Desiderio Pinto, Luana Cremascoli and Roberta De Santis for administrative assistance. Dr. Alice Colombo is supported by the 37th cycle PhD programme in "Scienze farmacologiche biomolecolari, sperimentali e cliniche", Università degli Studi di Milano. Dr. Elsa Franchi is supported by the 39th cycle PhD programme in "Scienze farmacologiche biomolecolari, sperimentali e cliniche", Università degli Studi di Milano.

## Appendix A. Supplementary data

Supplementary data to this article can be found online at <https://doi.org/10.1016/j.heliyon.2024.e31852>.

## References

- [1] W. Herrington, B. Lacey, P. Sherliker, J. Armitage, S. Lewington, Epidemiology of atherosclerosis and the potential to reduce the global burden of atherothrombotic disease, *Circ. Res.* 118 (2016) 535–546, <https://doi.org/10.1161/CIRCRESAHA.115.307611>.

- [2] P. Libby, P.M. Ridker, G.K. Hansson, Progress and challenges in translating the biology of atherosclerosis, *Nature* 473 (2011) 317–325, <https://doi.org/10.1038/nature10146>.
- [3] K.A. Campbell, M.J. Lipinski, A.C. Doran, M.D. Skafren, V. Fuster, C.A. McNamara, Lymphocytes and the adventitial immune response in atherosclerosis, *Circ. Res.* 110 (2012) 889–900, <https://doi.org/10.1161/CIRCRESAHA.111.263186>.
- [4] R. Gräbner, K. Lötzer, S. Döpping, M. Hildner, D. Radke, M. Beer, R. Spanbroek, B. Lippert, C.A. Reardon, G.S. Getz, et al., Lymphotoxin beta receptor signaling promotes tertiary lymphoid organogenesis in the aorta adventitia of aged ApoE<sup>-/-</sup> mice, *J. Exp. Med.* 206 (2009) 233–248, <https://doi.org/10.1084/jem.20080752>.
- [5] M.P.W. Moos, N. John, R. Gräbner, S. Nossmann, B. Günther, R. Vollandt, C.D. Funk, B. Kaiser, A.J.R. Habenicht, The lamina adventitia is the major site of immune cell accumulation in standard chow-fed apolipoprotein E-deficient mice, *Arterioscler. Thromb. Vasc. Biol.* 25 (2005) 2386–2391, <https://doi.org/10.1161/01.ATV.0000187470.31662.fe>.
- [6] E.W. Kienecker, H. Knoche, Sympathetic innervation of the pulmonary artery, ascending aorta, and coronar glomera of the rabbit. A fluorescence microscopic study, *Cell Tissue Res.* 188 (1978) 329–333, <https://doi.org/10.1007/BF00222641>.
- [7] C. Cavallotti, P. Bruzzone, M. Mancone, Catecholaminergic nerve fibers and beta-adrenergic receptors in the human heart and coronary vessels, *Heart Ves.* 17 (2002) 30–35, <https://doi.org/10.1007/s003800200039>.
- [8] C.M. Noller, A.J. Mendez, A. Szeto, M. Bouliana, M.M. Llabre, J. Zaias, N. Schneiderman, P.M. McCabe, Structural remodeling of sympathetic innervation in atherosclerotic blood vessels: role of atherosclerotic disease progression and chronic social stress, *Psychosom. Med.* 79 (2017) 59–70, <https://doi.org/10.1097/PSY.0000000000000360>.
- [9] S.K. Mohanta, L. Peng, Y. Li, S. Lu, T. Sun, L. Carnevale, M. Perrotta, Z. Ma, B. Förstera, K. Stanic, et al., Neuroimmune cardiovascular interfaces control atherosclerosis, *Nature* 605 (2022) 152–159, <https://doi.org/10.1038/s41586-022-04673-6>.
- [10] C.A. Maggi, S. Manzini, G. Grimaldi, S. Evangelista, A. Meli, High-cholesterol diet induces altered responsiveness of rabbit arterial smooth muscle to noradrenaline, *Pharmacology* 30 (1985) 273–280, <https://doi.org/10.1159/000138078>.
- [11] A.L. Stewart-Lee, J. Aberdeen, G. Burnstock, Sympathetic neurotransmission in the Watanabe heritable hyperlipidaemic rabbit mesentery artery, *Cardiovasc. Res.* 25 (1991) 1035–1041, <https://doi.org/10.1093/cvr/25.12.1035>.
- [12] P. Karoon, G. Burnstock, Reduced sympathetic noradrenergic neurotransmission in the tail artery of Donryu rats fed with high cholesterol-supplemented diet, *Br. J. Pharmacol.* 123 (1998) 1016–1021, <https://doi.org/10.1038/sj.bjp.0701719>.
- [13] J. Abd Alla, Y. El Faramawy, U. Quitterer, Microarray gene expression profiling reveals antioxidant-like effects of angiotensin II inhibition in atherosclerosis, *Front. Physiol.* 4 (2013) 148, <https://doi.org/10.3389/fphys.2013.00148>.
- [14] F. Arnaboldi, M. Busnelli, L. Cornaghi, S. Manzini, C. Parolini, F. Dellera, G.S. Ganzetti, C.R. Sirtori, E. Donetti, G. Chiesa, High-density lipoprotein deficiency in genetically modified mice deeply affects skin morphology: a structural and ultrastructural study, *Exp. Cell Res.* 338 (2015) 105–112, <https://doi.org/10.1016/j.yexcr.2015.07.032>.
- [15] M. Busnelli, S. Manzini, A. Colombo, E. Franchi, F. Bonacina, M. Chiara, F. Arnaboldi, E. Donetti, F. Ambrogi, R. Oleari, et al., Lack of ApoA-I in ApoEKO mice causes skin xanthomas, worsening of inflammation, and increased coronary atherosclerosis in the absence of hyperlipidemia, *Arterioscler. Thromb. Vasc. Biol.* 42 (2022) 839–856, <https://doi.org/10.1161/ATVBAHA.122.317790>.
- [16] C.A. Schneider, W.S. Rasband, K.W. Eliceiri, NIH Image to ImageJ: 25 years of image analysis, *Nat. Methods* 9 (2012) 671–675, <https://doi.org/10.1038/nmeth.2089>.
- [17] M. Busnelli, S. Manzini, F. Bonacina, S. Soldati, S.S. Barbieri, P. Amadio, L. Sandrini, F. Arnaboldi, E. Donetti, R. Laaksonen, et al., Fenretinide treatment accelerates atherosclerosis development in apoE-deficient mice in spite of beneficial metabolic effects, *Br. J. Pharmacol.* 177 (2020) 328–345, <https://doi.org/10.1111/bph.14869>.
- [18] S. Manzini, M. Busnelli, C. Parolini, L. Minoli, A. Ossoli, E. Brambilla, S. Simonelli, E. Lekka, A. Persidis, E. Scanziani, et al., Topiramate protects apoE-deficient mice from kidney damage without affecting plasma lipids, *Pharmacol. Res.* 141 (2019) 189–200, <https://doi.org/10.1016/j.phrs.2018.12.022>.
- [19] S. Manzini, C. Pinna, M. Busnelli, P. Cinquanta, E. Rigamonti, G.S. Ganzetti, F. Dellera, A. Sala, L. Calabresi, G. Franceschini, et al., Beta2-adrenergic activity modulates vascular tone regulation in lecithin:cholesterol acyltransferase knockout mice, *Vasc. Pharmacol.* 74 (2015) 114–121, <https://doi.org/10.1016/j.vph.2015.08.006>.
- [20] M. Busnelli, S. Manzini, M. Chiara, A. Colombo, F. Fontana, R. Oleari, F. Potì, D. Horner, S. Bellosta, G. Chiesa, Aortic gene expression profiles show how ApoA-I levels modulate inflammation, lysosomal activity, and sphingolipid metabolism in murine atherosclerosis, *Arterioscler. Thromb. Vasc. Biol.* 41 (2021) 651–667, <https://doi.org/10.1161/ATVBAHA.120.315669>.
- [21] S. Manzini, M. Busnelli, A. Colombo, E. Franchi, P. Grossano, G. Chiesa, reString: an open-source Python software to perform automatic functional enrichment retrieval, results aggregation and data visualization, *Sci. Rep.* 11 (2021) 23458, <https://doi.org/10.1038/s41598-021-02528-0>.
- [22] M.W. Pfaffl, A new mathematical model for relative quantification in real-time RT-PCR, *Nucleic Acids Res.* 29 (2001) e45, <https://doi.org/10.1093/nar/29.9.e45>.
- [23] A.M. Bolger, M. Lohse, B. Usadel, Trimmomatic: a flexible trimmer for Illumina sequence data, *Bioinformatics* 30 (2014) 2114–2120, <https://doi.org/10.1093/bioinformatics/btu170>.
- [24] D. Kim, G. Pertea, C. Trapnell, H. Pimentel, R. Kelley, S.L. Salzberg, TopHat2: accurate alignment of transcriptomes in the presence of insertions, deletions and gene fusions, *Genome Biol.* 14 (2013) R36, <https://doi.org/10.1186/gb-2013-14-4-r36>.
- [25] D. Szklarczyk, A.L. Gable, K.C. Nastou, D. Lyon, R. Kirsch, S. Pyysalo, N.T. Doncheva, M. Legeay, T. Fang, P. Bork, et al., The STRING database in 2021: customizable protein-protein networks, and functional characterization of user-uploaded gene/measurement sets, *Nucleic Acids Res.* 49 (2021) D605–D612, <https://doi.org/10.1093/nar/gkaa1074>.
- [26] B.T. Sherman, M. Hao, J. Qiu, X. Jiao, M.W. Baseler, H.C. Lane, T. Imamichi, W. Chang, DAVID: a web server for functional enrichment analysis and functional annotation of gene lists (2021 update), *Nucleic Acids Res.* 50 (2022) W216–W221, <https://doi.org/10.1093/nar/gkac194>.
- [27] S.K. Mohanta, C. Yin, C. Weber, A.J.R. Habenicht, Neuroimmune cardiovascular interfaces in atherosclerosis, *Front. Cell Dev. Biol.* 11 (2023) 1117368, <https://doi.org/10.3389/fcell.2023.1117368>.
- [28] C. Parolini, M. Busnelli, G.S. Ganzetti, F. Dellera, S. Manzini, E. Scanziani, J.L. Johnson, C.R. Sirtori, G. Chiesa, Magnetic resonance imaging visualization of vulnerable atherosclerotic plaques at the brachiocephalic artery of apolipoprotein E knockout mice by the blood-pool contrast agent B22956/1, *Mol. Imag.* 13 (2014), <https://doi.org/10.2310/7290.2014.00012>.
- [29] A. Gisterà, D.F.J. Ketelhuth, S.G. Malin, G.K. Hansson, Animal models of atherosclerosis-supportive notes and tricks of the trade, *Circ. Res.* 130 (2022) 1869–1887, <https://doi.org/10.1161/CIRCRESAHA.122.320263>.
- [30] M.S. Duncan, R.S. Vasani, V. Xanthakis, Trajectories of blood lipid concentrations over the adult life course and risk of cardiovascular disease and all-cause mortality: observations from the framingham study over 35 years, *J. Am. Heart Assoc.* 8 (2019) e011433, <https://doi.org/10.1161/JAHA.118.011433>.
- [31] K. Fronck, J.D. Turner, Combined effect of cholesterol feeding and sympathectomy on the lipid content in rabbit aortas, *Atherosclerosis* 37 (1980) 521–528, [https://doi.org/10.1016/0021-9150\(80\)90059-3](https://doi.org/10.1016/0021-9150(80)90059-3).
- [32] K. Kacem, G. Bonvento, J. Seylaz, Effect of sympathectomy on the phenotype of smooth muscle cells of middle cerebral and ear arteries of hyperlipidaemic rabbits, *Histochem. J.* 29 (1997) 279–286, <https://doi.org/10.1023/a:1026418413313>.
- [33] K. Kacem, C. Sercombe, M. Hammami, E. Vicaut, R. Sercombe, Sympathectomy causes aggravated lesions and dedifferentiation in large rabbit atherosclerotic arteries without involving nitric oxide, *J. Vasc. Res.* 43 (2006) 289–305, <https://doi.org/10.1159/000093010>.
- [34] R. Hachani, H. Dab, M. Sakly, E. Vicaut, J. Callebert, R. Sercombe, K. Kacem, Chemical sympathectomy induces arterial accumulation of native and oxidized LDL in hypercholesterolemic rats, *Auton. Neurosci.* 166 (2012) 15–21, <https://doi.org/10.1016/j.autneu.2011.08.008>.
- [35] R. Hachani, H. Dab, M. Sakly, R. Sercombe, J. Callebert, E. Vicaut, K. Kacem, The profile of the extracellular matrix changes in the aorta after sympathectomy in the hypercholesterolemic rats, *Auton. Neurosciences* 164 (2011) 67–73, <https://doi.org/10.1016/j.autneu.2011.07.005>.